Electronic Supplementary Material (ESI) for ChemComm.

Electronic Supplementary Information

Multitasking Polyamine/Ferrioxalate Nano-Sized Assemblies: Thermo-, Photo-, and Redox-Responsive Soft Materials Made Easy

Santiago E. Herrera[a], Maximiliano L. Agazzi[a], M. Lorena Cortez[a], Waldemar A. Marmisollé[a], Mario Tagliazucchi[b,*], Omar Azzaroni[a,*].

[a.] *Instituto de Investigaciones Fisicoquímicas Teóricas y Aplicadas (INIFTA), (UNLP, CONICET), Sucursal 4, Casilla de Correo 16, 1900 La Plata, Argentina.*

[b.] *Departamento de Química Inorgánica, Analítica y Química Física, INQUIMAE, CONICET. Facultad de Ciencias Exactas y Naturales. Ciudad Universitaria, Pabellón 2, Buenos Aires C1428EHA, Argentina*

Experimental procedure

PEI/FeOx Polyamine-salt aggregate (PEI/FeOx-PSA) formation

PEI/FeOx-PSAs were obtained by mixing aqueous solutions of potassium ferrioxalate dihydrate (FeOx) (synthesized in our lab) and polyethylenimine (PEI) (branched, Mw=10000, purchased from Polysciences). A PEI solution (14 ml, 0.33 mg/ml – 7.67 mM NH_2) deoxygenated by Ar bubbling and adjusted to pH=4.5 was placed in a 50 ml beaker. Then, under continuous magnetic stirring (50 rpm), 10 ml of deoxygenated FeOx solution (0.9 mg/ml - 1.83 mM) at pH=4.5 was quickly added in order to avoid heterogeneous formation of PSAs. The as-prepared colloidal dispersion (0.76 mM FeOx and 0.192 mg/ml PEI) was bubbled with Ar during 30 min and stored tightly closed in dark for 24 h at 20 °C.

Zeta potential measurements

Zeta potential measurements were carried out with a ZetaSizer Nano (ZEN3600, Malvern, U.K.) at 20 °C using a DTS1060 disposable cuvettes. Particle zeta potential was obtained from the electrophoretic mobility with a Laser Doppler Velocimetry using a general purpose analysis model.

Dynamic light scattering (DLS) measurements

DLS measurements were carried out with a ZetaSizer Nano (ZEN3600, Malvern, U.K.) using a quartz cuvette with a screw cap to prevent contamination with molecular oxygen. All measurements were collected using a 173° backscatter angle with 10 runs (20 sec run^{-1}), fixed sensor position (1.25 mm), and non-fixed filter attenuation. For the PSA characterization and light response experiments, the temperature was set to 20 °C.

Transmission electron microscopy (TEM) measurements

Images were obtained with a LaB6-TEM of type JEOL JEM-1400PLUS (120 kV) equipped with a GATAN US1000 CCD camera (2 k x 2 k). Samples were stained with phosphotungstic acid on carbon grids to create contrast. Particle diameter analysis was conducted using ImageJ 1.52a software.

Atomic Force Microscopy (AFM) measurements

AFM measurements (EC-AFM, Agilent 5500 AFM/SPM) were carried out in contact mode using a triangular Silicon tip PointProbe® Plus (PPP-CONT, Nanosensors) with a typical force constant of 0.2 N/m. A drop of a PEI/FeOx-PSA was placed over a clean highly oriented pyrolytic graphite (HOPG) substrate. After 5 minutes of PSA adsorption, the liquid drop was removed and the substrate was gently dried under a stream of nitrogen. Image analysis was performed with Gwyddion 2.5 software (http://gwyddion.net/).

IR measurements

Chemical characterization of the PEI/FeOx-PSA was performed with Fourier Transformation Infrared Spectroscopy (FITR). In order to remove the free PEI and FeOx, a PSA solution was centrifuged and the precipitate was re-suspended by sonication. FTIR measurements were performed using a Varian 600 FTIR spectrometer from KBr pellets.

Determination of the PSA stoichiometry

The PEI:FeOx molar ratio inside the PSA structure was determined indirectly by UV-Vis spectroscopy. A colloidal dispersion of PEI/FeOx PSAs was prepared by mixing 8 ml of PEI 8.44 mM (using a molar monomer mass of 43 g mol^{-1}) and 4 ml of FeOx 7.33 mM. After 24 h of stabilization, the colloid was centrifuged (10000 rpm) for 30 min and the supernatant was collected for analysis. All solutions were prepared in acetate buffer (0.2 M) at pH=5.80.

Quantification of FeOx in the supernatant: The concentration of FeOx in the supernatant was obtained by UV-Vis spectroscopy forming a red coloured complex ($[Fe(bpy)_3]^{2+}$) and measuring the absorbance at λ=522 nm according to Dallinger's method.[1] Briefly, 1.00 ml of a 1:20 dilution of the supernatant was mixed with 1.00 ml of a solution containing 2,2'-Bipyridine (0.8 mM) and ascorbic acid (0.25 mM). The absorbance at λ=522 nm was registered and the FeOx concentration was obtained by means of a calibration curve using a FeOx stock solution. All solutions were prepared in acetate buffer (0.2 M) at pH=5.80.

Quantification of PEI in the supernatant: The concentration of PEI was obtained by UV-Vis spectroscopy forming a blue coloured complex between PEI and Cu^{2+} and measuring the absorbance at λ=620 nm according to previous reports.[2,3] Briefly, 1.00 mL of concentrated NaOH was added to a 5.00 ml aliquot of PSA supernatant, raising the pH to about pH=13. The solution was centrifuged to remove the $Fe(OH)_3$ formed during the NaOH addition. Following, the pH of a 5.00 ml aliquot was lowered to pH=5.80 by addition of concentrated HCl. Then, the volume was completed up to 6.00 ml with buffer solution. Finally, 1.00 ml of this solution was mixed with 1.00 ml of a 100 mM $CuSO_4$ solution. The absorbance at λ=620 nm was registered and the PEI concentration was obtained by means of a calibration curve using a PEI stock solution. All solutions were prepared in acetate buffer (0.2 M) at pH=5.80.

UV-Vis spectroscopy measurements

UV-Vis experiments were carried out using a Perkin Elmer Lambda 35 spectrometer. All PEI/FeOx-PSA spectra were measured between 700 and 350 nm using a quartz cuvette with a screw cap (5 ml, 1-cm path length) at 20 °C.

Light-response experiments

Light-response experiments were carried out using a combination of UV-Vis and DLS measurements at 20 °C. To avoid Fe(II) oxidation, the PEI/FeOx-PSA sample was placed in a tight-closed screw-cap quartz cuvette completely filled (5 ml). For homogeneous light irradiation, a small stir bar was introduced into the cuvette. Then, under continuous stirring, the sample was exposed to 40 s of UV light using a UV fluorescent tube (8 W, Interelec, model TL2001-8W) placed at 1 cm oriented parallel to the cuvette. After UV exposure, the sample was analyzed by UV-Vis and DLS. Irradiation/measurement cycles were repeated until no appreciable absorption was detected at λ=580 nm.

Redox-response experiments

For the redox-response experiments, a quartz cuvette was filled with 2 ml of a PEI/FeOx-PSA colloidal dispersion. Then, 50 µl of an aqueous solution of ascorbic acid (Sigma-Aldrich) at different concentrations (205 mM, 41 mM, 4.1 mM and 0.41 mM) was placed into the cuvette. Immediately after the addition of ascorbic acid, the time course of the sample extinction at λ=580 nm was recorded. All experiments were conducted in dark.

Temperature-response experiments

We placed a 2-ml aliquot of PEI/FeOx-PSA colloidal dispersion in a closed screw-cap quartz cuvette and analyzed the sample by DLS as a function of temperature. The sample was initially cooled to 5 °C and stabilized for 2 h. Then, consecutive measurements were conducted changing the temperature in intervals of 5 °C, going up to 55 °C. Between each measurement, we allowed the sample to stabilize for 5 minutes at constant temperature.

To construct the plot of PEI/FeOx-PSA colloidal-threshold ratio vs. temperature (Figure 4b) two aqueous solutions of PEI (0.33 mg/ml, pH=4.5) and FeOx (0.9 mg/ml, pH=4.5) were thermostatted at the desired temperature. Then, 2 ml of PEI solution was placed in a thermostatted small beaker and a dropwise addition of FeOx solution was carried out until turbidity was detected.

Supporting data

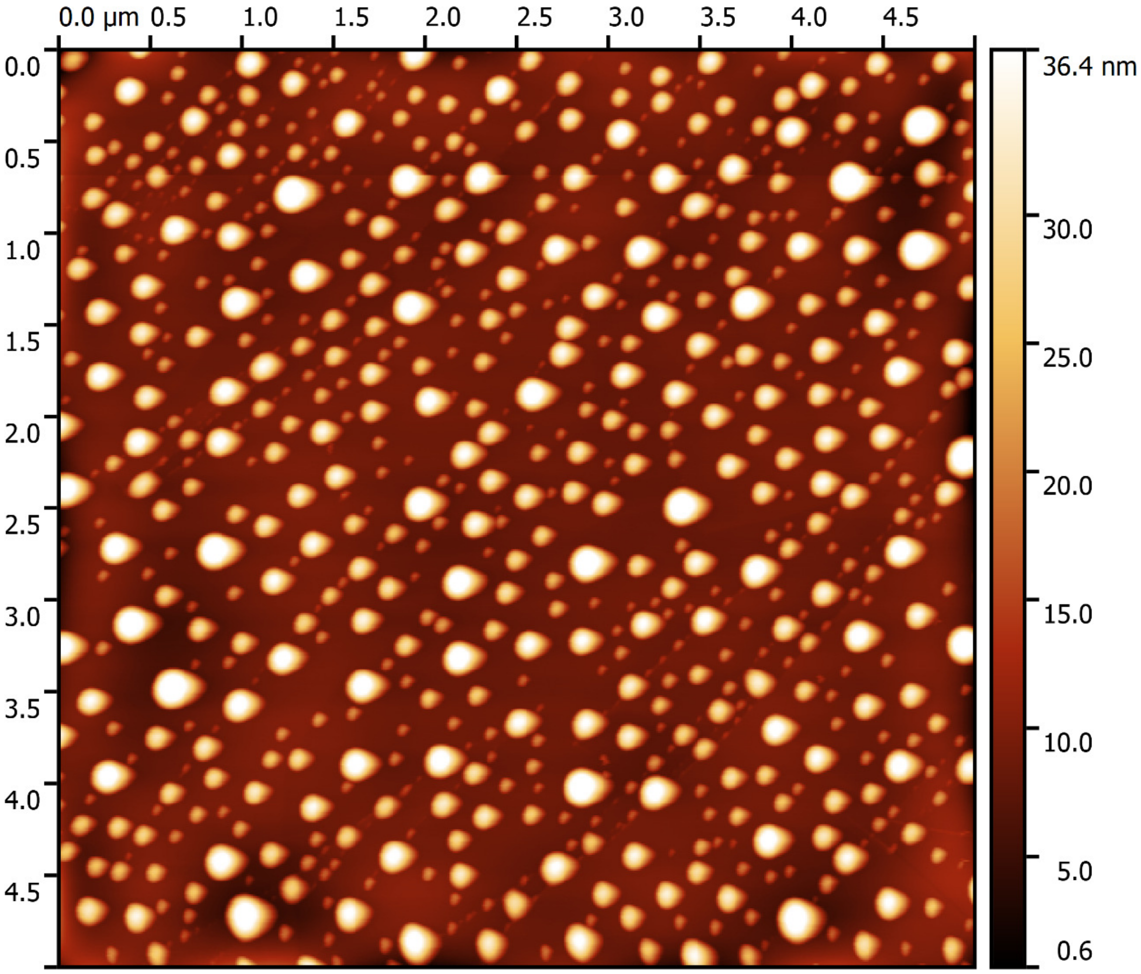

Figure S1. AFM topography image of PEI/FeOx-PSAs adsorbed on top of HOPG.

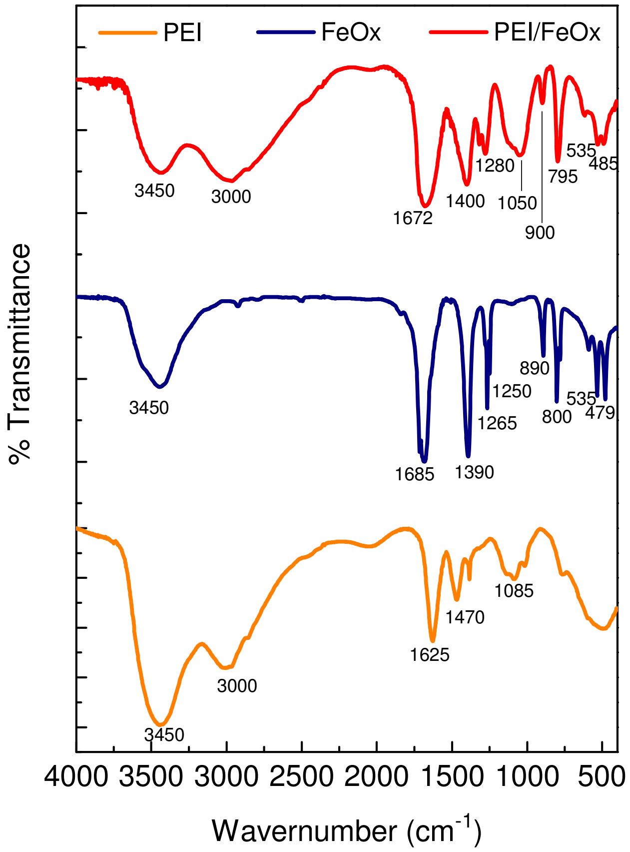

Figure S2. FTIR spectra of PEI (bottom panel), FeOx (middle panel) and PEI/FeOx-PSAs (upper panel).

Figure S2 shows the FTIR spectra (4000 to 400 cm^{-1}) of PEI, FeOx and PEI/FeOx-PSA. For PEI (orange line), the broad band centered around 3450 cm^{-1} can be assigned to N-H stretching vibration. The signal centered at 3000 cm^{-1} corresponds to C-H stretching vibration. Bands at 1625 cm^{-1} and 1470 cm^{-1} correspond to N-H and C-H bending vibrations, respectively. Signals between 980 and 1350 cm^{-1} can be assigned to C-N stretching vibration. The FTIR spectrum of FeOx (blue line) presents characteristic absorption bands of the iron oxalate complex.[4–7] The stretching oxalate modes appeared at 1685 cm^{-1} (C=O) and 1390 cm^{-1} (C-O). Signals at 1265 cm^{-1} and 1250 cm^{-1} are due to contributions of C-O (stretching vibration) and O-C=O (bending vibration). The C-C symmetric stretching mode of oxalates ligands and O-C-O deformational mode are observed at 890 cm^{-1} and 800 cm^{-1}, respectively. Bands observed at 535 and 479 cm^{-1} can be assigned to Fe–O stretching vibrations. The broad band centered around 3450 cm^{-1} corresponds to O-H stretching vibration of coordinated water molecules.

The PEI/FeOx-PSA spectrum (red line) clearly exhibits a combination of the spectra of the individual building blocks previously described. The typical bands of PEI appear on the spectrum of PSA. The presence of FeOx in the crosslinked matrix is confirmed by the typical signals at 485, 535, 795, 900 and 1672 cm^{-1}. The small shifts observed in some PSA signals compared to the peaks of the individual components are probably due to the interactions between PEI and FeOx.

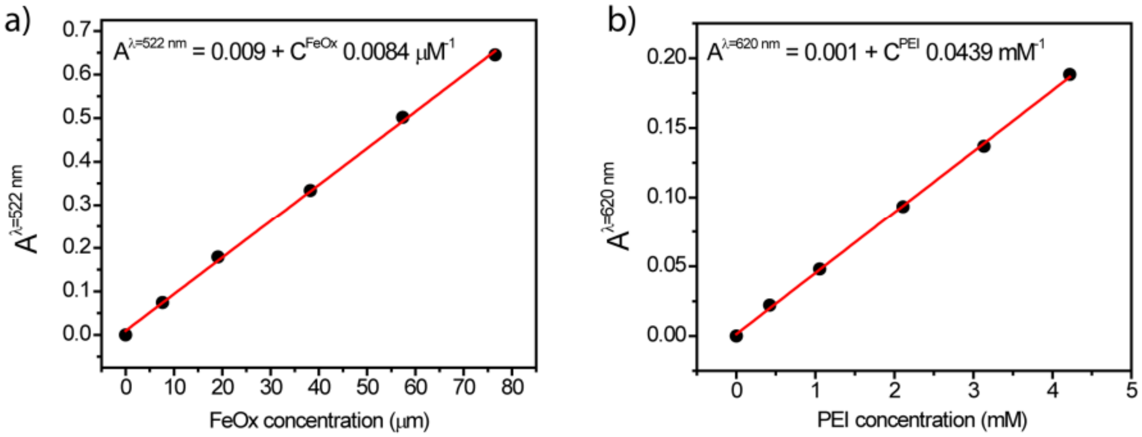

Figure S3. UV-Vis spectroscopy calibration curves for quantification of FeOx (a) and PEI (b).

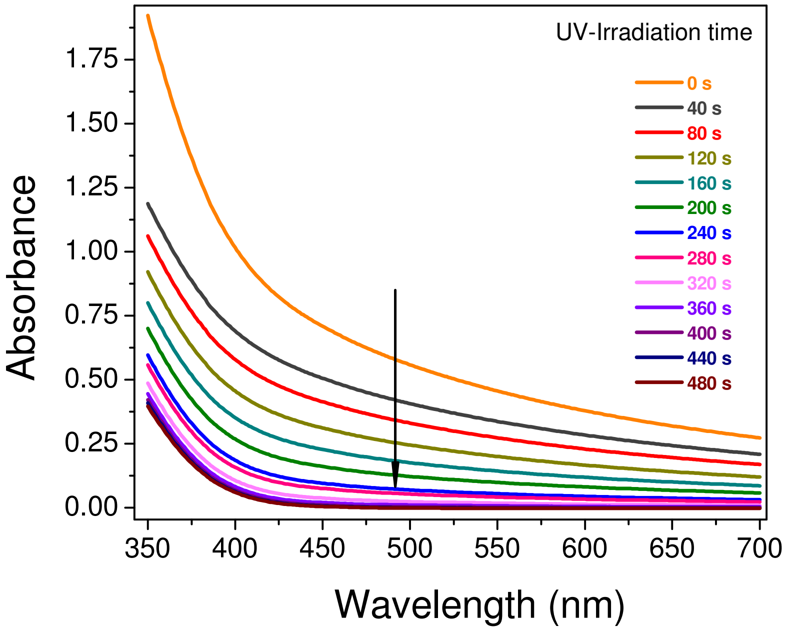

Figure S4. Photoinduced dissolution of PEI/FeOx-PSAs. UV-Vis spectra of a PEI/FeOx-PSA sample after irradiation with UV light for increasing times.

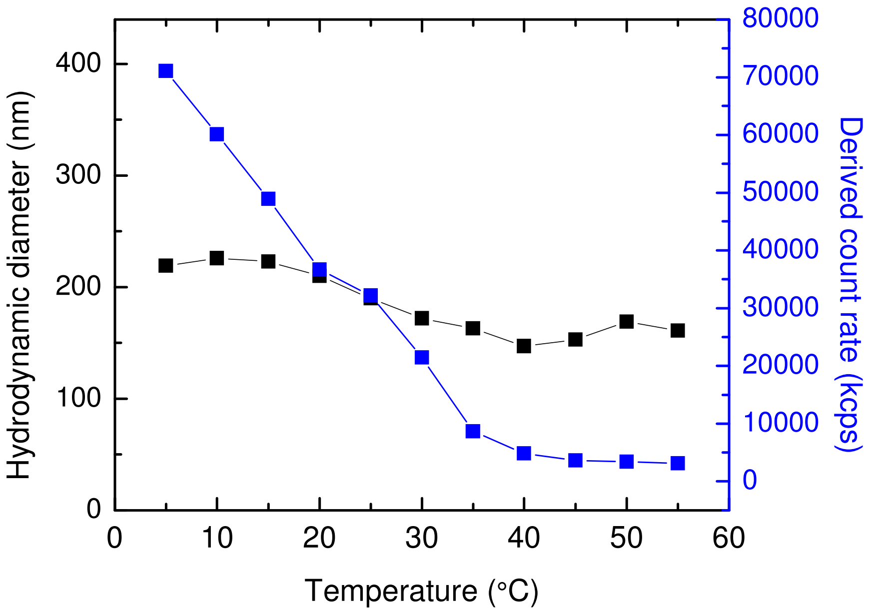

Figure S5. Temperature response. DLS measurements of a PEI/FeOx-PSA sample ([FeOx]/[PEI]=1.95) at different temperatures. Drived count rate (right axis) and particle hydrodynamic diameter (left axis) in the 5 to 55 °C scan. DLS sensor position: 1.25 mm.

References:

1 R. F. Dallinger, *J. Chem. Educ.*, 1995, **72**, 936.

2 T. D. Perrine and W. R. Landis, *J. Polym. Sci. Part A-1 Polym. Chem.*, 1967, **5**, 1993–2003.

3 T. Wen, F. Qu, N. B. Li and H. Q. Luo, *Arab. J. Chem.*, 2017, **10**, S1680–S1685.

4 J. Fujita, A. E. Martell and K. Nakamoto, *J. Chem. Phys.*, 1962, **36**, 324–331.

5 M. Narsimhulu and K. A. Hussain, *IOP Conf. Ser. Mater. Sci. Eng.*, 2018, **360**, 012048.

6 M. C. D'Antonio, A. Wladimirsky, D. Palacios, L. Coggiolaa, A. C. González-Baró, E. J. Baran and R. C. Mercader, *J. Braz. Chem. Soc.*, 2009, **20**, 445–450.

7 Y. Duan, J. C. Waerenborgh, J. M. Clemente-Juan, C. Giménez-Saiz and E. Coronado, *Chem. Sci.*, 2017, **8**, 305–315.